Tail Aggregation and Domain Diffusion in Ionic Liquids

Yanting Wang and Gregory A. Voth*

Center for Biophysical Modeling and Simulation and Department of Chemistry, University of Utah, 315 South 1400 East Room 2020, Salt Lake City, Utah 84112-0850

Received: May 24, 2006; In Final Form: July 15, 2006

An extended multiscale coarse-graining model for ionic liquids is used to investigate the liquid crystal-like phase in certain ionic liquids. The tail groups of the cations with a sufficient side-chain length are found to aggregate, forming spatially heterogeneous domains, due to the competition between the electrostatic interactions between the charged head groups and the anions and the collective short-range interactions between the neutral tail groups. With a sufficiently long alkyl chain at a low enough temperature, the tail domains remain relatively stable, despite the diffusion of individual ions in the liquid phase. With increasing temperature, the average tail domains begin to diffuse, while beyond a transition temperature, their average density has an almost uniform distribution, although the tail groups still form instantaneous domains.

1. Introduction

Although ionic liquids have gained wide attention as one of the new solvents to achieve "green chemistry", many of their basic physical properties still remain unknown. Generally the cations of ionic liquids are composed of a charged head group with nearly unit net charges and a nonpolar tail group of an alkyl side chain with little charge. Because of atomic polarization, when the side chain is short, the tail group has an effective nonzero partial charge. With increasing side-chain length, the partial charges on the alkyl chain approach zero. The interactions between the head groups and the anions are then dominated by electrostatic interactions, while the nonpolar parts of the side chain interact mainly through the collective short-range interactions. The competition between these two kinds of interactions having different length scales ensures that ionic liquids in general do not behave as a simple liquid.

Both experiments[1−4] and simulations[5−8] have found that the side-chain length has an influence on the physical properties of ionic liquids, and a liquid crystal-like phase has been observed for pure ionic liquids with long side chains.[9−12] Nevertheless, no systematic mechanisms have been proposed to explain these phenomena, so the study of the physical properties of ionic liquids with various side-chain lengths is of great interest. In addition, it is well-known that amphiphilic molecules form micelles in solvents (see, e.g., refs 13−15). Some experiments[16,17] have been carried out which study the micelle formation of ionic liquids in solvents. Several experiments[18,19] have also studied surfactant aggregation in ionic liquids. However, the characteristics of pure ionic liquids *without* solvents are also not well understood.

Recently a multiscale coarse-graining (MS-CG) approach[20,21] has been successfully applied to the $EMIM^+/NO_3^-$ ionic liquid.[22] The MS-CG model of ionic liquids allows for large systems to be simulated for long times, thus revealing features of the system that are difficult to see with conventional all-atom MD simulations. The MS-CG model for the $EMIM^+/NO_3^-$ ionic liquid was also extended to study the physical properties of ionic liquids when varying their alkyl chain lengths.[8] With these MS-CG models, it has been found that, with sufficient long side chains, the tail groups of the cations aggregate to form spatially heterogeneous tail domains. Atomistic MD simulations have subsequently confirmed this finding.[23,24]

In this paper, more results from the molecular dynamics (MD) simulations by using the MS-CG models are reported to reveal qualitatively how the cationic alkyl side-chain length influences the structural and dynamical properties of this class of ionic liquid. Due to the simplicity of the MS-CG model, qualitative rather than quantitative results are given by the MS-CG MD simulations, which are expected to be quantitatively different from atomistic MD results.[24] However, by comparing the experimental and simulation results, we will show that the MS-CG model captures the essential interactions in ionic liquids. Considering the computational demands of all-atom MD, the MS-CG models have an advantage over the more precise all-atom MD approach for the qualitative study of the physical properties for ionic liquids.

In the MS-CG simulations, it is found that, at a suitable temperature and with enough attractive interactions between the nonpolar groups on the cationic side chain, the tail groups form relatively stable tail domains, despite the ionic diffusion in the liquid phase. However, at high enough temperatures, the tail groups are expected to have sufficient thermal energy so that they no longer aggregate. The transition from the heterogeneous phase to the homogeneous phase was investigated by slowly heating the ionic liquids. It was found that this transition is not characterized by the behavior of individual tail groups, but rather the collective behavior of the tail domains. With increasing temperature but still below the transition point, the tail domains diffuse and smear out, but the central positions of the domains remain relatively unchanged. At temperatures above but not far from the transition point, the tail groups still aggregate simultaneously, but the tail domains diffuse through the whole space with an almost uniform probability. At very high temperatures, the tail groups are no longer able to aggregate, and therefore distribute almost homogeneously.

The tail aggregation and domain diffusion mechanisms described above seem likely to be general for most ionic liquid

* To whom correspondence should be addressed. Phone: (801)581-7272. Fax: (801)581-4353. E-mail: voth@chem.utah.edu.

10.1021/jp063199w CCC: $33.50
Published on Web 08/24/2006

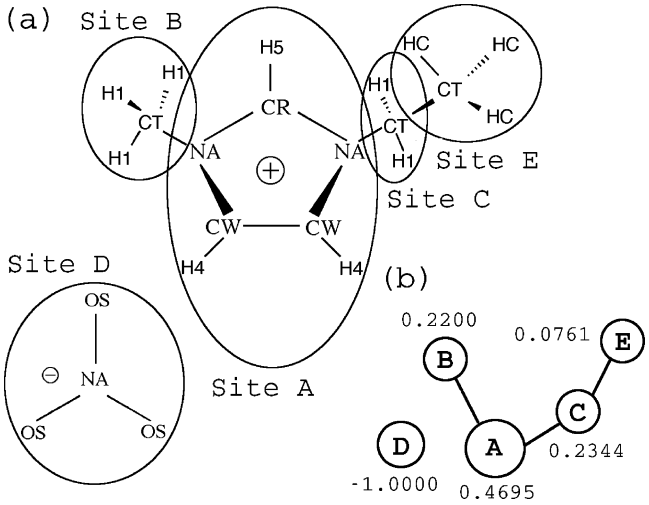

Figure 1. (a) Atomic and (b) multiscale coarse-grained $EMIM^+/NO_3^-$ ionic liquid structures. The numbers shown on the coarse-grained sites are their partial charges.

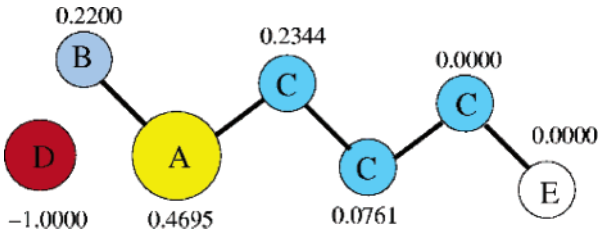

Figure 2. Multiscale coarse-grained model of $BMIM^+/NO_3^-$ (C_4). The number on each coarse-grained site is the assigned partial charge for this site.

systems, independent of the molecular details, e.g., the identity of the ions. Other physical properties, such as micelle formation and solubility of ionic liquids, might also be influenced by the tail aggregation phenomenon. These features are also expected to help in the systematic design of ionic liquid systems to meet the requirements of key applications.

2. Methods

In this section the method of building the extended MS-CG models is described. A heterogeneity order parameter is also defined to quantify the spatial heterogeneity in ionic liquids.

2.1. Multiscale Coarse-Graining Model for Ionic Liquids. The $EMIM^+/NO_3^-$ ionic liquid has been extensively studied by both the nonpolarizable[25] and the polarizable[26,27] atomistic MD models at a fixed temperature of 400 K. The atomistic models are very time-consuming, so they are not suitable for simulating large systems for long times at multiple temperatures. A MS-CG approach[20,21] has thus been adopted to construct a coarse-grained model for ionic liquids.[22] This approach derives the pairwise effective potentials from the underlying polarizable atomistic interactions. The 23 atoms in one ion pair are reduced to 5 CG sites. The atomic and CG structures for the $EMIM^+/NO_3^-$ ionic liquid are shown in Figure 1. The bonded forces between CG sites were obtained from the configurational data from the polarizable atomistic MD simulations, while the short-range nonbonded forces between CG sites were force-matched by an extended least-squares force-matching approach.[28] The CG sites also have long-range Coulomb interactions between them, with their partial charges assigned to the sum of the partial charges of their underlying atoms. The force field parameters for the MS-CG model are given in ref 22 and the Supporting Information associated with it.

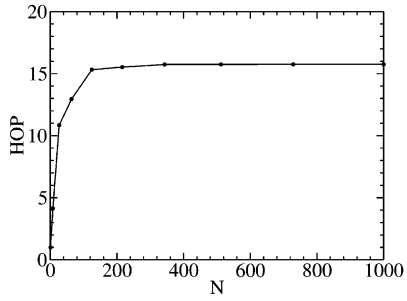

Figure 3. Heterogeneity order parameters computed for various numbers of particles ideally homogeneously distributed in a cubic box with periodic boundary conditions applied.

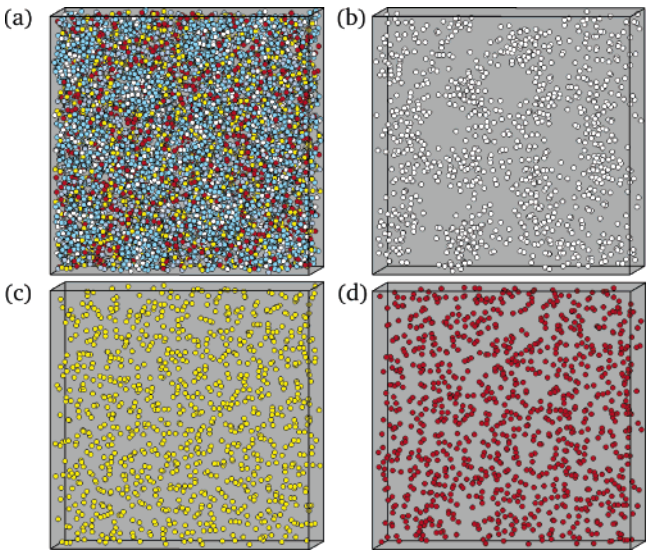

Figure 4. One snapshot of C_4 with 1000 ion pairs at $T = 700$ K with (a) all atoms, (b) tail groups only, (c) head groups only, and (d) anions only.

With the MS-CG approach, the many-body electronic polarizability is successfully incorporated into effective pairwise interactions. With a virial constraint fixing the system pressure, the MS-CG models also rebuild satisfactory structural and thermodynamic properties. However, it should be noted that the diffusion for the MS-CG model is faster than the atomistic models, and the nonbonded effective potentials have limited transferability between different temperatures. In the following simulations, the diffusion and temperatures therefore provide only a *relative* comparison to help qualitatively understand the general trends of the behavior of the ionic liquid systems.

The MS-CG model was then extended to study the ionic liquids with different side-chain lengths of cations. For convenience, the ionic liquid systems will be denoted by the number of carbons on the alkyl chain, e.g., $EMIM^+/NO_3^-$ as C_2 and $BMIM^+/NO_3^-$ as C_4. To construct C_1, Site C in the CG model for $EMIM^+/NO_3^-$ is eliminated and its partial charge is added to Site E. For the C_3, C_4, C_6, and C_8 systems, appropriate numbers of Sites C representing methylene groups are inserted between Site C and Site E of C_2. The partial charge of the first C site is assigned to be that for the E site of C_2. The remaining C sites and the E site are assigned a zero partial charge. The extra bonded force field parameters other than those in the C_2 system are assigned with the parameters for sp^3 carbon (CT) sites given in ref 29. The MS-CG model for the C_4 system is shown in Figure 2. Below the term "tail group" will specifically refer to Site E, "head group" will refer to Site A, and "anion" will be Site D.

2.2. Heterogeneity Order Parameter. A simple method to identify the spatial heterogeneity for identical sites is to divide the simulation space into small cells and count the number of sites in each cell. The spatial heterogeneity is thus characterized by an uneven distribution of site densities in different cells. One disadvantage of this method is the discontinuity caused when the sites move across the cell boundaries. This discontinuity may cause significant errors when the number of available particles in each cell is small. Alternatively, a new order parameter is defined here to quantify the spatial heterogeneity continuously. This Gaussian-like *heterogeneity order parameter* (HOP) is defined for each site as

$$h_i = \sum_j \exp(-r_{ij}^2/2\sigma^2) \tag{1}$$

where r_{ij} is the modulation of the vector $\mathbf{r}_i - \mathbf{r}_j$ corrected with the periodic boundary conditions, $\sigma = L/N^{1/3}$, with L the side length of the cubic simulation box, and N is the total number of sites.

The average HOP is computed by averaging over all N_S sites of interest, such that

$$h = \frac{1}{N_S}\sum_{i=1}^{N_S} h_i \tag{2}$$

The HOP is defined so that it is topologically invariant with the absolute distances between sites. Because the weights of the sites far from the central site decrease quickly with distance, the HOP approaches a constant with increasing number of sites. Some ideal systems with $N = n^3$, $n = 1, 2, 3, ...$, sites homogeneously distributed in a cubic box were constructed, and the HOP was computed for these systems with periodic boundary conditions applied. The values are plotted in Figure 3. From this plot it can be seen that the HOP approaches a constant value of 15.7496 after $N \geq 729$.

2.3. Lattice Heterogeneity Order Parameter. The HOP defined above characterizes the spatial heterogeneity of the distribution of the tail groups. In section 3.3 it will be shown that it is the behavior of the tail domains, not the behavior of the individual tail groups, characterizing the phase transition of the tail aggregation phenomenon. Thus defining a lattice HOP that quantifies the average spatial heterogeneity of the tail domains, rather than the individual tail groups, is necessary.

For each configuration, only tail groups (CG Sites E) are consided, and the HOP is computed for each tail site by eq 1. The cubic simulation box is then divided into small cubic cells. The lattice HOP c_i for cell i is the HOP averaged over all tail groups in this cell, such that

$$c_i = \frac{1}{M}\sum_{j=1}^{M} h_{ij} \tag{3}$$

where M is the number of tail groups in cell i and h_{ij} is the HOP of the jth tail group in cell i.

Due to the limited number of available tail groups, in one configuration some cells inside the tail domain may not include any sites for calculating their HOP value. This can be justified by the HOP values of their neighboring cells. If a cell contains no tail groups, the lattice HOP is conveniently taken as the average value of all neighboring cells with a weight as the inverse of the center−center distance, such that

$$c_i = \frac{\sum_j \frac{1}{r_{ij}} c_{ij}}{\sum_j \frac{1}{r_{ij}}} \tag{4}$$

where c_{ij} is the lattice HOP of the jth neighbor of cell i and r_{ij} is the distance from the center of cell i to the center of cell j. Neighboring cells are defined as the cells with their center−center distance from cell i less than a cutoff. In this case the cutoff is chosen to be 5.9 Å, the distance of the minimum between the first and second peaks in the tail−tail RDF plot for the C_4 system with 64 ion pairs, as shown in Figure 5a.

The set of the lattice HOP $\{c_i\}$ for one instantaneous configuration represents the instantaneous distribution of the tail groups, thus the tail domains. The average lattice HOP $\bar{c}_i$ for cell i, which characterizes the ensemble average of the behavior of the tail domains, is obtained by averaging over c_i in the same cell position in all of the saved configurations at the given temperature. The average HOP for the whole system is then obtained by averaging over all average lattice HOPs in the system, given by

$$\bar{c} = \frac{1}{N_C}\sum_{i=1}^{N_C} \bar{c}_i \tag{5}$$

where N_C is the number of cells in the system. The average HOP may serve as an order parameter to quantify the phase transition.

3. Results

The MS-CG models for ionic liquids at $T = 400$ and 700 K were used to perform the MD simulation for the ionic liquid systems by using the DL_POLY program[30] with the time step of 1 fs. For all different size and chain length systems, the manually constructed initial configurations first went through a constant *NPT* simulation by a Hoover barostat[31] with a pressure of 1 atm to equilibrate and obtain the average volume. A constant *NVT* simulation by a Nosé−Hoover thermostat[32] with the average volume obtained from the *NPT* run then followed to collect data.

3.1. Tail Aggregation. The C_4 MS-CG system with 64, 216, 512, and 1000 ion pairs underwent a 1 ns *NVT* MD simulation after a 1 ns *NPT* MD simulation at $T = 700$ K. Figure 4 shows one snapshot of the simulation for the C_4 system with 1000 ion pairs. It can be seen that the tail groups of the cations aggregate to form several spatially heterogeneous tail domains, while the head groups and the anions distribute relatively homogeneously. Visual examination confirms that this tail formation also exists for the other three sizes.

The radial distribution functions (RDF) were then computed for tail groups (Site E) to characterize this spatial heterogeneity. Figure 5 shows the RDFs calculated for the individual CG Sites E for the C_4 systems with those four sizes. The very high first peak (around 6) in the tail−tail RDF and its second peak (around 2) close to the first peak indicate the aggregation of tail groups. In contrast, the highest peaks for the head groups and the anions are only around 1.5, so compared to the tail groups, the head groups and the anions are much more uniformly distributed. Except that the smaller size systems are a little more ordered than the larger ones, the RDFs do not show noticeable finite size effects. Thus the smallest simulation systems of 64 ion pairs seem valid to qualitatively describe the general trends of C_4.

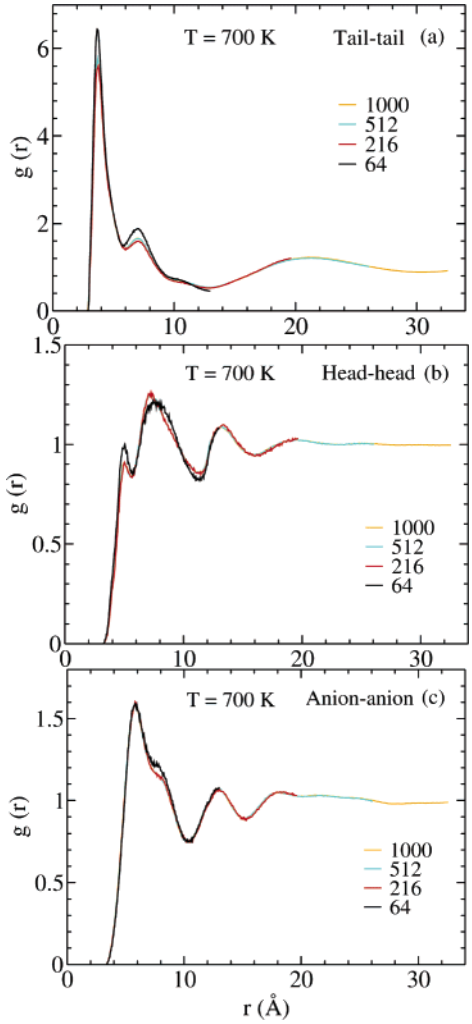

Figure 5. Radial distribution functions for single sites (a) tail−tail (E−E), (b) head−head (A−A), and (c) anion−anion (D−D) of the C_4 systems with several system sizes at $T = 700$ K.

The C_1, C_2, C_3, C_6, and C_8 systems with 64 ion pairs were then simulated at $T = 700$ K, following the same procedure as C_4. The RDFs were shown as Figure 4 in ref 8. The tail−tail RDFs for C_1 and C_2 demonstrate that no spatial heterogeneity exists in these two systems. By contrast, those for C_6 and C_8 have the two similar characteristic high peaks as that for C_4, showing the heterogeneous distributions of tail groups. The RDF for C_3 has a first high peak of 3 that is about half the height for C_4, but no second high peak. This suggests that, at $T = 700$ K, C_3 is above but close to the transition point. For the cation−cation RDF, the characteristic peak at about 4 Å is due to the parallel packing of the planar-like head groups.[8,26] From the anion−anion RDFs, it is clear that the anions distribute close to the head groups.

The spatially heterogeneous distribution of the tail groups was also characterized by the HOP calculations. Figure 6 shows the HOPs for the tail groups, head groups, and anions for different side-chain length systems with 64 ion pairs. For C_1 and C_2, the HOPs for the tail groups are almost the same as those for the head groups and the anions. For C_4, C_6, and C_8, the HOPs for the head groups and anions are only a little larger than those for C_1 and C_2, showing that they still distribute homogeneously. By contrast, the HOPs for the tail groups are much larger than those for the head groups and the anions, indicating that the tail groups distribute quite heterogeneously.

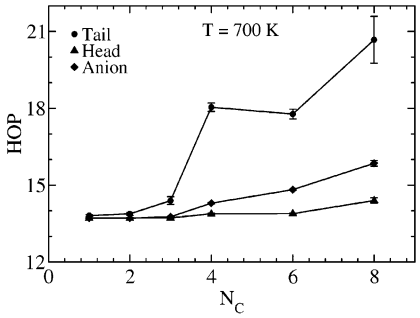

Figure 6. Heterogeneity order parameters for the tail groups, head groups, and anions with different alkyl chain lengths with 64 ion pairs at $T = 700$ K.

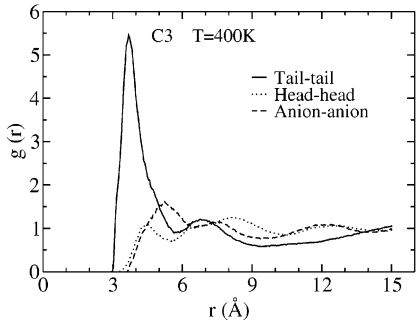

Figure 7. Single-site radial distribution functions for the C_3 system with 125 ion pairs at $T = 400$ K.

The results for C_3 are between the above two groups, in agreement with the RDF results.

The equilibrated configurations with 64 ion pairs for different chain length systems at $T = 700$ K were also simulated at $T = 400$ K with the corresponding MS-CG model at that temperature. For C_3 and C_4, the side lengths of the simulation boxes with 64 ion pairs shrink to be smaller than twice the cutoff length for short-range interactions of 12.17 Å, so a simulation with 125 ion pairs was performed instead for these two systems. The C_1 and C_2 systems still show no strong aggregation (data not shown), while the single site RDFs for C_3 shown in Figure 7 clearly show that C_3 exhibits tail aggregation. This suggests that the transition for C_3 occurs at a temperature between 400 and 700 K. The structures of the C_4, C_6, and C_8 systems are very similar to those at $T = 700$ K (data not shown).

3.2. Mechanism for the Tail Aggregation. The tail aggregation may be understood by noting that the cations have a positively charged head group and a neutral tail group. The collective short-range interactions between the charged groups are very small compared to the Coulomb interactions around the equilibrium distance, so that the local structures are determined mainly by the partial charges on those sites. By contrast, the neutral tail groups do not have the Coulomb interactions between them. Their equilibrium distances are determined only by their collective short-ranged interactions. In ionic liquids, the short-range equilibrium distances are smaller than those for the charged groups. The two kinds of interactions compete with each other under a geometrical constraint between the head groups and the tail groups. When the alkyl chain is short, the whole cation acts more like one charged single site, and the equilibrium distance between cations is determined mainly by the head groups. When the chain is sufficiently long, although the strong Coulomb interactions still require the head groups and the anions to maintain their local structures, the tail groups are comparatively far from the head groups, so the Coulomb interactions on the head groups have less influence

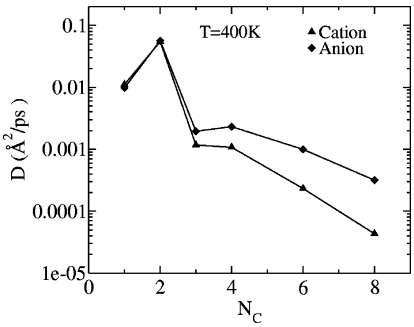

Figure 8. Diffusion constants for the systems with different alkyl chain lengths with 125 ion pairs at $T = 400$ K.

on the aggregation of the tail groups. The tail groups therefore have more freedom to be closer to each other, due to their collective short-range interactions. In addition, longer side chains have more collective short-range attractive interactions between them. At low temperatures, when the collective short-range attractive interactions between the side chains are larger than the thermal energy, the tail groups form relatively stable tail domains. With increasing temperature, when a larger degree of entropy sets in, the tail domains are expected to smear out and the tail groups distribute more homogeneously. The behavior of the aggregated tail domains at higher temperatures will be discussed in section 3.3.

With this tail aggregation mechanism in mind, many experimental results can be qualitatively explained. The different local structures with different equilibrium distances for the tail groups and the charged groups result in a liquid crystal-like structure closely related to those observed in the experiments.[9−12] The experimentally observed heterogeneity, however, is on a mesoscopic scale for a lamellar structure. More quantitative comparison can only be obtained when simulations are performed in a much larger scale than the current study.

With the same cations but an anion of $(CF_3SO_2)_2N^-$ different from the NO_3^- studied in this work, Tokuda et al.[3] reported experimental results that the summations of the diffusion coefficients for the cations and the anions follows the order $C_2 > C_1 > C_4 > C_6 > C_8$. Seddon et al.[1] and Huddleston et al.[2] reported similar experimental results for systems with different anions. The results from our MS-CG MD simulations agree with the above experimental observations. In Figure 8 the plot shows the diffusion coefficients D for the cations and the anions for the simulated systems at $T = 400$ K vs the number of carbons on the side chains. The diffusion coefficients were obtained by fitting the linear part of the mean square displacements with $6Dt$,[33] where t is the time interval. From C_2 to C_8, the collective short-range interactions in the tail domains retard the movement of the cations. Longer side chains have stronger collective short-range interactions, so the diffusion decreases with increasing side-chain length. The diffusion of the anions is associated with that of the cations, since they are attracted to be around the head groups of the cations. The diffusion constants of C_1 and C_3 are smaller than the trends for C_2, C_4, C_6, and C_8, showing that for some physical properties the ionic liquids with an odd number of carbons on the side chain are different from those with an even number of carbons.[11]

By virtue of MD simulations, Urahata and Ribeiro[7] found that the diffusion increases from C_1 to C_4, and then decreases when the side chain is longer. This is qualitatively consistent with the experiments and our simulations. The difference might be explained by the differences of the anions and the simulation model used. The MD simulations performed by Margulis[5] and Urahata and Ribeiro[6] found that the systems are more structured with longer side chains. These results are also consistent with our simulations, and can be explained by the inhomogeneous distribution of tail groups and slower diffusion with increasing side-chain length.

All of the above qualitative trends have been confirmed by our recent MD simulations[24] using a polarizable atomistic model. However, compared with the atomistic results, it is found that the extended MS-CG models give stronger attractive interactions between the side chains. Thus the MD simulations by the MS-CG models give an increasing mass density with increasing side-chain length, rather than a decreasing density found in the experiments[1−3] and in our atomistic MD simulations.

In our atomistic MD simulations,[24] as well as the earlier simulations of Lopes and Padua,[23] it is clear that the head groups and the anions always try to retain their local structures by varying their global distributions. Although this still seems true in the MS-CG simulations, because the volume of the simulation box increases very slowly with increasing alkyl chain length, the charged groups are also able to roughly maintain their global shapes in the MS-CG simulations. Thus the MS-CG model is not as accurate for studying the behavior of the head groups and the anions. However, the present level of the MS-CG model is still valuable for studying the behavior of the tail domains, as discussed below. More accurate and detailed MS-CG models will be presented in the future.

The atomistic MD models have significantly weaker attractions between the side chains. To have stable tail domains in the atomistic models, the side-chain lengths must be long (roughly beyond C_{12}), and the temperature must be rather low (approximately lower than 400 K). The long side chains require a very big simulation box size, and the low temperatures lead to a very slow dynamics. In our polarizable atomistic simulations,[24] a relatively large simulation size of 512 ion pairs still shows significant finite size effects for C_{10} (24 064 atoms) and C_{12} (27 136 atoms).[24] The atomistic MD simulations for these two systems already approach the limit of current computational abilities.

By contrast, the extended MS-CG model for C_4 already has a strong tail aggregation. Our results indicate that the very small size of 64 ion pairs does not show significant finite size effects for C_4. Moreover, the dynamics of the MS-CG model is faster than that of the corresponding atomistic model. The phase transition temperature for the tail domains is therefore expected to be further from the glass transition and the melting temperatures. Thus the phase behavior of the tail domains can be studied with less interference from the glass transition or the melting transition. Although the simulation results from the extended MS-CG model will be quantitatively different from the atomistic results, the qualitative mechanism obtained from these studies will be valuable for guiding future simulation and experimental work.

3.3. Domain Diffusion. The results for C_3 described previously suggest that, at higher temperatures, the increasing thermal energy attenuates the intensity of tail aggregation. It is expected that, at high temperatures, the entropy is so large that the tail groups cannot form domains anymore. It is therefore of great interest to study the nature of this transition.

An intuitive mechanism for the tail domain transition is that, with increasing temperatures, it occurs when the tail groups change from distributing heterogeneously (aggregation to form tail domains) to distributing homogeneously. The C_4 system with its MS-CG model at $T = 700$ K was selected to test this conjecture, since it is the shortest tail system having strong tail group aggregation with an even number of carbons on the side

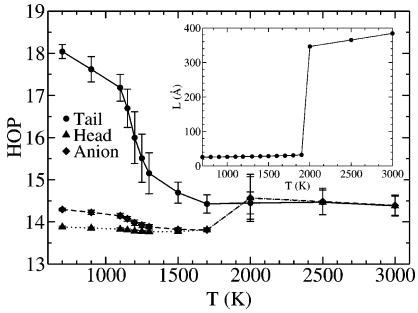

Figure 9. Heterogeneity order parameters vs temperature for the tail groups, head groups, and anions for the C_4 system with 64 ion pairs. The inset is the plot of the average side lengths of the simulation box vs temperature, showing that the system goes through a liquid−gas transition at about $T = 2000$ K.

chains, and it forms stable tail domains at $T = 700$ K, while the diffusion is fast enough to ensure that the system is still in a liquid state. It needs to be emphasized again that the temperatures reported below only have a qualitative, rather than quantitative, meaning.

The C_4 system with 64 ion pairs was heated from $T = 700$ K up to 3000 K over many steps. At each step the system went through a constant *NPT* simulation for 1 ns to equilibrate, followed by a 1 ns constant *NVT* simulation to collect data. The system goes through a liquid-to-gas transition at about $T = 2000$ K, as shown by the side length of the cubic simulation box plotted in the inset of Figure 9. It should be noted that the transition temperatures in these MS-CG studies are quite high because of the too strong tail interactions compared to the atomistic case, as discussed earlier. Also, real ionic liquids would be likely to thermally decompose at some of the temperatures studied in this qualitative model.

The average HOP (eqs 1 and 2) was then computed for the tail groups, the head groups, and the anions at each temperature and is shown in Figure 9. The average HOPs for the head groups and the anions do not change much in the whole temperature range. In the gas phase, on average the sites should distribute more uniformly than in the liquid phase. However, because large thermal fluctuations in the gas phase result in instantaneous local fluctuations, therefore local spatial heterogeneity, the average HOPs in the gas phase are a little larger than those in the liquid phase. At $T = 700$ K, the average HOP for the tail groups has a large value of 18, showing a very inhomogeneous distribution of tail groups. Visual examination confirms that, while the individual cations change their positions from time to time, the formed tail domains are relatively stable. The HOP decreases linearly until $T = 1100$ K, because the increasing thermal energy attenuates the tail aggregation, and therefore smears the intensity of the tail groups in the domains. From $T = 1100$ K to 1700 K, the HOP for the tail groups decreases exponentially, approaching smoothly the value in the gas phase.

According to the HOPs shown in Figure 9, it seems reasonable to assume that the domains formed by the tail groups simply diffuse with increasing temperature, and finally disappear at a very high temperature, when the tail groups distribute uniformly. The calculations of the caloric curve (potential energy vs temperature) and the specific heat vs temperature described below show that the above argument may be invalid for ionic liquids and, in fact, there may exist an actual phase transition.

The caloric curve in Figure 10 shows a linear increase of the potential energy at the temperatures below $T = 1140$ K and above 1230 K, respectively. Between these two temperatures the potential energy increases with a larger slope, indicating a

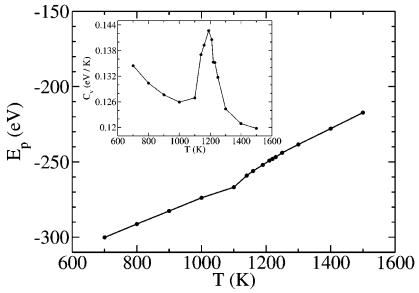

Figure 10. Caloric curve and the constant-volume specific heat (inset) vs temperature for the C_4 system with 64 ion pairs.

phase transition in this temperature range. In addition to the slope change for the caloric curve, generally a peak in the specific heat vs temperature plot signals a phase transition. The constant-volume specific heat capacity in the canonical ensemble can be calculated from the potential energy fluctuations[33] by

$$C_v = \frac{(\langle E_p^2 \rangle - \langle E_p \rangle^2)}{k_B T^2} + \frac{3}{2} N k_B \qquad (6)$$

where k_B is Boltzmann's constant, T is the system temperature, E_p is the potential energy, and N is the number of CG sites in the system.

The inset of Figure 10 shows the specific heat plot for the C_4 system with 64 ion pairs. There exists a peak with its maximum at the critical transition temperature of about $T_c = 1200$ K, consistent with the results from the caloric curve. These results do not agree with the mechanism suggested above that the tail groups simply change from distributing heterogeneously to homogeneously gradually from $T = 1100$ to 1700 K. Instead, the results suggest that a more complex mechanism governs the tail aggregation transition.

By closer visual examination of the saved configurations, it seems that at high temperatures the tail domains do not simply diffuse and smear with relatively stable central positions, but they move considerably and even dissolve and reorganize to form different tail domains. This suggests that the transition is not simply reflected by the behavior of the individual tail groups, but the overall tail domains. To study the global behavior of the tail domains, the lattice HOPs described in section 2.3, showing the ensemble averaged heterogeneity, were then computed, to study the transition from the point of view of the tail domains.

The sets of the average lattice HOPs $\{\bar{c}_i, i = 1...N_C\}$ for the C_4 system with 64 ion pairs at different temperatures are shown in Figure 11. For each temperature, the cubic simulation box is divided into $N_C = 512$ small cubic cells, with 8 cells along each side. In each figure, one small sphere is assigned to the center of each cell, with its color representing the average lattice HOP in this cell. The scale in Figure 11 shows the mapping from the magnitudes of HOP to the colors. The coldest color represents 0, meaning no tail groups ever stay in this cell; the warmest color represents the magnitudes larger than 18, indicating that the tail groups have a very heterogeneous distribution in this cell. The magnitudes between are evenly divided and represented by different colors ranging from cold to warm.

At $T = 700$ K, well below $T_c = 1200$ K, many cells have an average lattice HOP of 0, and the remainder have a very large magnitude. This illustrates that the tail domains are very stable and have a fixed position, despite the fact that the system is in a liquid state, so that the tail groups diffuse and move around

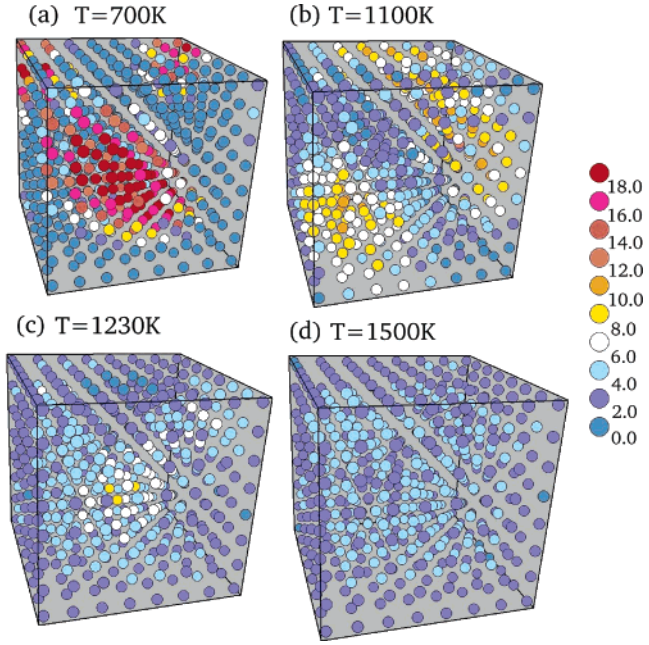

Figure 11. Lattice heterogeneity order parameters in each cell at different temperatures for the C_4 system with 64 ion pairs.

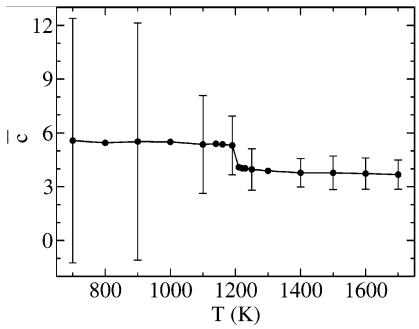

Figure 12. Average lattice heterogeneity order parameters vs temperature for the C_4 system with 64 ion pairs.

in the tail domains. At $T = 1100$ K, just below T_c, the tail domains diffuse and smear, with less intense heterogeneity. At $T = 1230$ K, just above T_c, the tail domains are so smeared out that the tail groups are almost free to enter any part of the simulation box. At $T = 1500$ K, well above T_c, the average lattice HOPs in the cells are almost identical, indicating that, on average, the tail groups have equal probabilities to visit any position in the simulation box. The aggregated tail domains are poorly defined at this high temperature.

The average HOPs for the whole simulation box $\bar{c}$ defined in eq 5 were then computed at different temperatures and are plotted in Figure 12. The error bars are the standard deviations, showing how the magnitudes differ from cell to cell. Below T_c, with increasing temperature, the average HOP does not change much, while the standard deviation becomes smaller because of the smearing of the tail domains. The average HOP then drops sharply at T_c. At the temperatures above T_c, the average HOP and its standard deviation change little, showing that, on average, the tail groups distribute almost homogeneously.

To explain the difference between the average HOPs for individual tail groups shown in Figure 9 (defined by eq 2) and those for tail domains shown in Figure 12 (defined by eq 5) the average lattice HOPs for three instantaneous configurations at $T = 1230$ K, just above $T_c = 1200$ K, are calculated and shown in Figure 13. It can be clearly seen that, at this temperature, the tail groups still aggregate to form instantaneous tail domains. So in the instantaneous configurations, the tail groups still distribute very heterogeneously. The average HOPs shown in Figure 9 reflect this *instantaneous* heterogeneity. Nevertheless, the tail domains move around freely from time to time, so *on average* the tail domains distribute almost uniformly, as illustrated in Figure 11c.

According to the above results, a mechanism for the phase transition of tail domains is suggested as the following. At very low temperatures, but above the bulk glass transition or melting transition point, the tail domains formed by the aggregated tail groups are relatively stable, forming the "solid" domains, despite the fact that the ions diffuse in the liquid phase, so that the tail groups move around in the tail domains from time to time. With increasing temperatures below the transition point T_c, due to higher thermal energy, the tail domains diffuse and smear out, but the centers of the domains stay in a relatively fixed position. When the temperature is a little higher than T_c, the tail groups still aggregate to form tail domains instantaneously, but the tail domains no longer stay in a fixed position. In other words, the tail domains are "melted". On average the tail domains have a nearly uniform probability to appear in any position throughout the whole space. At these temperatures, while the instantaneous heterogeneity still exists, the ensemble average shows a spatial homogeneity. At very high temperatures far from T_c, the thermal energy is so large that the tail groups can hardly aggregate to form even instantaneous tail domains. The system is instantaneously homogeneous and behaves more like a simple liquid.

The above mechanism suggests that the transition of ionic liquids from a heterogeneous liquid to a homogeneous one is characterized by the behavior of the tail domains, namely the group behavior of the tail groups as a whole, rather than the behavior of the individual tail groups. Since the potential energy and the average lattice HOP seem to change continuously around the transition temperature, as shown in Figures 10 and 12, respectively, the phase transition of tail domains appears to be a second-order one. However, more work needs to be done to determine the order of this transition.

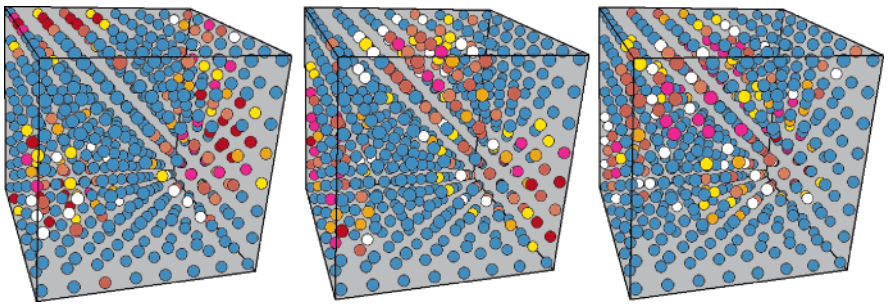

Figure 13. Lattice heterogeneity order parameters for three instantaneous configurations of the C_4 system with 64 ion pairs at $T = 1230$ K, just above the transition temperature of about 1200 K. The color scheme is the same as that shown in Figure 11.

4. Discussion and Conclusions

A MS-CG model for the $EMIM^+/NO_3^-$ ionic liquid has been extended to study the influence of cationic alkyl chain length on the structural and dynamic properties of ionic liquids. With sufficiently long side chains, the tail groups of the cations have been found to aggregate to form spatially heterogeneous tail domains. This can be understood by the competition of the collective short-range interactions between the tail groups and the long-range Coulomb interactions between the head groups and the anions. The physical picture gained from the MS-CG models also provides a qualitative explanation for certain experimental results. The aggregation behavior of the tail groups might be the reason that the ionic liquids form mesoscopic liquid crystal-like structures, as well as their higher viscosity and slower diffusion with longer side-chain length.

The extended MS-CG models exhibit stronger tail aggregation than the atomistic MD models. Nevertheless, the MS-CG model is still valuable as a qualitative model to grasp the essential physics for the side-chain length effects, and to qualitatively study the phase transition of the tail domains in ionic liquids.

With increasing temperature, the aggregated tail domains diffuse and smear out, and they finally form a homogeneous distribution of tail groups. However, this transition is not characterized by the behavior of individual tail groups, but the behavior of the tail domains as a whole, from being more solidlike below the transition point to more liquidlike above it. Above the transition temperature, although the tail groups may still aggregate instantaneously, on average the tail domains move around the whole space with an almost uniform probability.

Although the MS-CG simulations were carried out only for the imidazole-based ionic liquids with a nitrate anion, and the temperatures and the diffusion constants do not agree quantitatively with the all-atom MD simulations, the tail aggregation and domain diffusion phenomena are expected to form a general qualitative framework for most ionic liquids. Careful experimental selections of cation/anion combinations and side-chain length of cations might "tune" the desired phases of interest, such as the liquidlike domain phase, to exist in a range of application temperatures.

It is certainly necessary to verify and add more details to our proposed tail aggregation and domain diffusion mechanism with all-atom MD simulations. However, this is very difficult with current computational limitations. More advanced techniques will need be employed to accomplish this task. Such all-atom MD simulations will also help to address the unknown question of the role the charged groups play in the phase transition of the tail domains, or if they have their own phase behavior separate from the tail domains. It will also be very interesting to study the phase behavior of ionic liquids within a theoretical framework, given the competition of interactions on different lengths scales, similar to the work on stripe glasses[34] and oil/water separation.[35] This will be the subject of future research in our group.

Acknowledgment. This research was supported by the Air Force Office of Scientific Research (FA9550-04-1-0381). The authors thank Dr. Vinod Krishna, Dr. Yujie Wu, and Dr. Jhih-Wei Chu for useful discussions. Allocations of computer time from the National Center for Supercomputing Applications (NCSA) and the Center for High Performance Computing at the University of Utah are gratefully acknowledged.

References and Notes

(1) Seddon, K. R.; Stark, A.; Torres, M.-J. Alternative Media for Chemical Reactions and Processing. In *Clean Solvents*; ACS Symp. Ser. 819; Abraham, M., Moens, L., Eds.; American Chemical Society: Washington, DC, 2002.

(2) Huddleston, J. G.; Visser, A. E.; Reichert, W. M.; Willauer, H. D.; Broker, G. A.; Rogers, R. D. *Green Chem.* **2001**, *3*, 156.

(3) Tokuda, H.; Hayamizu, K.; Ishii, K.; Bin Hasan Susan, M. A.; Watanabe, M. *J. Phys. Chem. B* **2005**, *109*, 6103.

(4) Wakai, C.; Oleinikova, A.; Ott, M.; Weingärtner, H. *J. Phys. Chem. B* **2005**, *109*, 17028.

(5) Margulis, C. J. *Mol. Phys.* **2004**, *102*, 829.

(6) Urahata, S. M.; Ribeiro, M. C. C. *J. Chem. Phys.* **2004**, *120*, 1855.

(7) Urahata, S. M.; Ribeiro, M. C. C. *J. Chem. Phys.* **2005**, *122*, 024511.

(8) Wang, Y.; Voth, G. A. *J. Am. Chem. Soc.* **2005**, *127*, 12192.

(9) Lee, K. M.; Lee, C. K.; Lin, I. J. B. *Chem. Commun.* **1997**, 899.

(10) Gordon, C. M.; Holbrey, J. D.; Kennedy, A. R.; Seddon, K. R. *J. Mater. Chem.* **1998**, *8*, 2627.

(11) Holbrey, J. D.; Seddon, K. R. *J. Chem. Soc., Dalton Trans.* **1999**, 2133.

(12) Lee, C. K.; Huang, H. W.; Lin, I. J. B. *Chem. Commun.* **2000**, 1911.

(13) Smit, B.; Esselink, K.; Hilbers, P. A. J.; Os, N. M. v.; Rupert, L. A. M.; Szleifer, I. *Langmuir* **1993**, *9*, 9.

(14) Palmer, B. J.; Liu, J. *Langmuir* **1996**, *12*, 746.

(15) Marrink, S. J.; Mark, A. E. *J. Am. Chem. Soc.* **2003**, *125*, 15233.

(16) Consorti, C. S.; Suarez, P. A. Z.; de Souza, R. F.; Burrow, R. A.; Farrar, D. H.; Lough, A. J.; Loh, W.; da Silva, L. H. M.; Dupont, J. *J. Phys. Chem. B* **2005**, *109*, 4341.

(17) Bowers, J.; Butts, C. P.; Martin, P. J.; Vergara-Gutierrez, M. C.; Heenan, R. K. *Langmuir* **2004**, *20*, 2191.

(18) Fletcher, K. A.; Pandey, S. *Langmuir* **2004**, *20*, 33.

(19) Anderson, J. L.; Pino, V.; Hagberg, E. C.; Sheares, V. V.; Armstrong, D. W. *Chem. Commun.* **2003**, 2444.

(20) Izvekov, S.; Voth, G. A. *J. Chem. Phys.* **2005**, *123*, 134105.

(21) Izvekov, S.; Voth, G. A. *J. Phys. Chem. B* **2005**, *109*, 2469.

(22) Wang, Y.; Izvekov, S.; Yan, T.; Voth, G. A. *J. Phys. Chem. B* **2006**, *110*, 3564.

(23) Lopes, J. N. A. C.; Pádua, A. A. H. *J. Phys. Chem. B* **2006**, *110*, 3330.

(24) Wang, Y.; Jiang, W.; Voth, G. A. *Book in Ionic Liquids*; ACS Symp. Ser., submitted.

(25) Del Pópolo, M. G.; Voth, G. A. *J. Phys. Chem. B* **2004**, *108*, 1744.

(26) Yan, T.; Burnham, C. J.; Del Pópolo, M. G.; Voth, G. A. *J. Phys. Chem. B* **2004**, *108*, 11877.

(27) Yan, T.; Burnham, C. J.; Wang, Y.; Gao, X.; Voth, G. A. *J. Phys. Chem. B.* Submitted for publication.

(28) Izvekov, S.; Parrinello, M.; Burnham, C. J.; Voth, G. A. *J. Chem. Phys.* **2004**, *120*, 10896.

(29) Cornell, W. D.; Cieplak, P.; Bayly, C. I.; Gould, I. R.; Merz, K. M.; Ferguson, D. M.; Spellmeyer, D. C.; Fox, T.; Caldwell, J. W.; Kollman, P. A. *J. Am. Chem. Soc.* **1995**, *117*, 5179.

(30) Forester, T. R.; Smith, W. *DL_POLY user manual*; CCLRC, Daresbury Laboratory: Daresbury, Warrington, UK, 1995.

(31) Melchionna, S.; Ciccotti, G.; Holian, B. L. *Mol. Phys.* **1993**, *78*, 533.

(32) Hoover, W. G. *Phys. Rev. A* **1985**, *31*, 1695.

(33) Allen, M. P.; Tildesley, D. J. *Computer Simulation of Liquids*; Clarendon Press: Oxford, UK, 1987.

(34) Schmalian, J.; Wolynes, P. G. *Phys. Rev. Lett.* **2000**, *85*, 836.

(35) Wu, S.; Westfahl, H., Jr.; Schmalian, J.; Wolynes, P. G. *Chem. Phys. Lett.* **2002**, *359*, 1.